Optical Engineering

OpticalEngineering.SPIEDigitalLibrary.org

Design and fabrication of additively manufactured aluminum mirrors

Songnian Tan
Yalin Ding
Yongsen Xu
Lei Shi

SPIE.

Songnian Tan, Yalin Ding, Yongsen Xu, Lei Shi, "Design and fabrication of additively manufactured aluminum mirrors," *Opt. Eng.* **59**(1), 013103 (2020), doi: 10.1117/1.OE.59.1.013103

Design and fabrication of additively manufactured aluminum mirrors

Songnian Tan,[a,b,c,*] Yalin Ding,[a,c] Yongsen Xu,[a,c] and Lei Shi[a,c]

[a]Chinese Academy of Sciences, Changchun Institute of Optics, Fine Mechanics and Physics, Changchun, China

[b]University of Chinese Academy of Sciences, Beijing, China

[c]Chinese Academy of Sciences, Key Laboratory of Airborne Optical Imaging and Measurement, Changchun, China

Abstract. To meet the increasing demand for practicality and rapidity of the optical components in aircraft folding optical systems, an aluminum mirror preparation method based on additive manufacturing (AM) technology is proposed. From the perspective of special processing technology for AM, a preparation process chain of additively manufactured mirrors is proposed to address limitations in the design process such as size, support, and connectivity constraints. First, the deposited mirror manufactured by AM technology is prepared. Second, the additively manufactured metal mirror is densified by the hot isostatic pressing process. Then, computer numerical control machining and single-point diamond turning is applied to realize the shape of the surface. Finally, the AM mirror is coated with the gold film. The experimental results show that the surface quality is 0.384λ (peak-to-valley method) and 0.093λ (root mean square method) ($\lambda = 632.8$ nm), and the mirror surface roughness (Ra) is better than 8 nm. After the mirror is subjected to thermal cycles, the surface accuracy does not change significantly, which essentially meets the requirements of the aviation environment adaptability and shows good potential for application in the infrared band. © *2020 Society of Photo-Optical Instrumentation Engineers (SPIE)* [DOI: 10.1117/1.OE.59.1.013103]

Keywords: lightweight mirror; additive manufacturing; AlSi10Mg alloy; hot isostatic pressing; surface quality.

Paper 191146 received Aug. 26, 2019; accepted for publication Dec. 23, 2019; published online Jan. 11, 2020.

1 Introduction

With the rapid development of aviation technology, the folding optical systems of photoelectric detection equipment in aircraft are developing to be more lightweight and offer higher resolutions and more specific requirements have been raised for the volume and weight of optical components such as the folding mirrors in the folding optical system. Aluminum alloy metal mirrors have been gradually introduced into optical systems, owing to their excellent features, such as short process cycle and efficient process technology, low weight, and the associated low material costs.[1–3] The traditional aluminum alloy metal mirror is processed by removing a part of the mirror material without affecting its external dimensions and structural integrity. The common structures of the mirrors after weight reduction are the semiclosed honeycomb or lattice structures after weight decrease.[4] The upper limit of processing removal is approximately 50%,[5] which makes it extremely difficult to achieve both high stiffness and low weight. With the increasing demands for practicality and speed of the folding optical system, it has become increasingly important to develop aluminum alloy mirrors that can meet the requirements of low weight, high rigidity, and wide environmental adaptability.

Therefore, for the optical components in the aircraft folding optical system, an AlSi10Mg material mirror preparation scheme based on the emerging additive manufacturing (AM) technology is proposed. The core of this scheme is the use of a new mirror material, AlSi10Mg, as

*Address all correspondence to Songnian Tan, E-mail: tansongnian@126.com

0091-3286/2020/$28.00 © 2020 SPIE

one selection for the materials to prepare metal mirrors. For selective laser melting (SLM), AM technology cannot be used in the preparation of large-diameter mirrors due to equipment and process limitations. However, the AlSi10Mg material can be used to form a stiffer structure, i.e., a closed backplate, and the AM technology can be used to develop small aperture mirrors.

SLM is an AM technology that uses a high-energy laser beam to melt metal powder along the laser path, such that the molten metal rapidly solidifies to form the designed structure.[6] The mirror manufactured using the SLM method is composed of AlSi10Mg powders.[7] A significant advantage of the additively manufactured mirror is the athermalization design of the whole system. The frame structure of the airborne photoelectric detection equipment is usually made of aluminum alloy material. The thermal expansion coefficient of the AlSi10Mg material is $21 \times 10^{-6}/°C$, which is similar to that of the traditional 6061 aluminum alloy material ($24 \times 10^{-6}/°C$).[8,9] Here, AlSi10Mg can achieve thermal matching with the frame structure. The athermalization design allows the system to change proportionally as the temperature changes, but the image quality remains unchanged. Another advantage of the additively manufactured mirror is that it can achieve higher stiffness and withstand higher bending moments and shear forces by enclosing the mirror backplate.[10] In addition, the additively manufactured mirror has the advantages of a short process cycle, high forming precision, and more complex internal lightweight structures,[11] which can meet the practicality and rapidity requirements of the aircraft folding optical system.

In recent years, there has been rapid advancement in the exploration and research of such technologies. The Fraunhofer Institute IOF in Germany proposed a concept for the additively manufactured metal mirror for applied optics and precision engineering. They combined complex flow paths throughout the interior of the entire mirror, which is one of the proposed applications in the field of liquid-cooled mirrors. They also investigated the application of AM technology on lightweight mirrors.[12] Dr. H. Philip Stahl of NASA presented a highly lightweight aspherical mirror using AM techniques in a report on advanced optical systems and manufacturing techniques.[13] Laser-selective sintering by AlSi10Mg powders produces a mirror with a 500-mm diameter. The mirrors are processed by the single-point diamond turning (SPDT) technique, and they can be used in multiple scientific fields, such as deep space optical communication and terrestrial planetary search. Corning incorporation uses AM technology to create a back-open, honeycomb, lightweight, high-performance aluminum mirror that achieves a 15-Å root mean square (RMS).[14,15] The internal lightweight structure of the M1/M3 module used in the three-mirror anastigmatic telescope is additively manufactured by AlSi40 powders, resulting in a 64% weight reduction.[16]

While there has been a strong research focus on the preparation of metal mirrors based on AM technology, research on additively manufactured metal mirrors has just begun. The majority of additively manufactured mirrors are used in aerospace applications or laboratory environments. To meet the requirements to adapt them to harsh aviation environments, thermal cycle experiments are performed in this study to validate the stability of the surface quality.

To demonstrate the feasibility of this manufacturing method, this paper discusses the design constraints of the additively manufactured metal mirrors in detail and proposes a process chain for the development of an additively manufactured metal mirror. The main focus of the study is the design and manufacture of a flat metal mirror of size 67 mm × 50 mm, which is used as a fast steering mirror (FSM) in the infrared optical system. The surface quality and roughness after the AM process and thermal cycles are also investigated.

2 Additively Manufactured Metal Mirror Design

2.1 *Additive Manufacturing Technology Process Constraints*

As an advanced special processing technology, AM technology also has special structural design requirements in the manufacturing process, and designers must follow the corresponding process requirements during the design process.

2.1.1 *Size constraints*

Dimensional constraints are common in traditional manufacturing processes, and the AM process is no different in this respect. An overly small size can result in a weak overall structure, and for the mirror under gravitational force, it would also result in insufficient surface stiffness and a change in the surface shape, which would make it unsatisfactory as per the requirements of the optical design. The processing equipment determines the maximum size of the workpiece. For the current SLM technology equipment, the minimum formation size of the AlSi10Mg material ranges from 0.3 to 0.4 mm. and the maximum size is 800 mm × 400 mm × 500 mm. In the design process for the workpiece, the size is determined based on the structural design and simulation results. The required dimensions can be determined if the simulation results satisfy the mechanical properties of the structure.

2.1.2 *Support constraints and support removal*

In the AM process, it is often necessary to add a support structure underneath the large cantilever structure to prevent structural collapse. The use of the support structure not only increases the printing time and cost but also results in processing difficulties during the later support structure removal stage.

Therefore, utilizing an optimized structural configuration and posture during processing would reduce the amount of the support material required and could even achieve a self-supporting structure.[17] This could effectively reduce manufacturing costs and speed up the manufacturing process. However, in certain cases, it is essential to add support structures to avoid collapse during the SLM process, and the support structures have to be removed after the preparation is complete. Thus, ease of removal of the support structure is required to complete the processing of the mirror.

2.1.3 *Connectivity constraints*

The connectivity constraints mandate that no closed space exists within the structure. After the SLM process, it is necessary to remove the unmelted powders that have not been exposed to the beam in the interior of the three-dimensional (3-D) printed structure.

For the mirror, if the backplate is open, the unmelted powders inside can be removed easily. However, the mirror backplate often needs to be closed to achieve greater stiffness. Therefore, all internal features require a connection to the outside of the mirror. This can consist of circular holes on the inner ribs. Hence, to ensure the removal of the unmelted powders, the inside structure of the mirror should have no completely closed spaces. Furthermore, if the structure contains closed spaces, the internal support structures, which are added to aid processing, are difficult to remove and often require secondary processing.

2.2 *Metal Mirror Design Based on Additive Manufacturing Technology*

A CAD 3-D model of a metal mirror is designed for the FSM, as shown in Fig. 1. The FSM is a key component that improves the system-transmitted accuracy in the optical system. The accuracy of the FSM system can be further improved by reducing the weight and moment of inertia and increasing the rigidity of the mirror. The mirror surface is flat, and the mirror is applied in the infrared optical system.

2.2.1 *Size constraints*

The designed aperture size of the metal mirror is 67 mm × 50 mm. According to the processing requirements of the AM technology, the minimum inner rib thickness of the metal mirror is 1.6 mm, and the corner radians are limited to 1 mm.

2.2.2 *Support constraints*

A support structure was added to process the mirror, as shown in Fig. 2. The mirror surface was positioned downward, and the mirror was supported by the external support structure

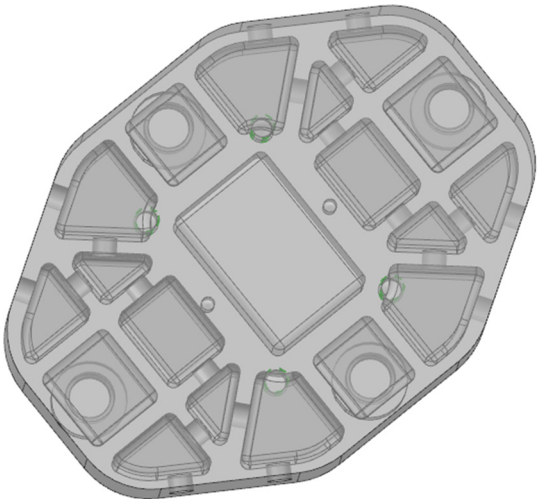

Fig. 1 CAD model of an additively manufactured aluminum mirror.

(blue portion). The angle between the mirror and the baseplate was maintained at 45 deg.[18] This could help the backplate of the mirror self-support and eliminate the need for additional support inside the mirror. Furthermore, this processing method could reduce the amount of material to be melted per layer as well as the internal stress of each layer. After the SLM process, the external support structure was removed using special processing methods such as wire cutting.

2.2.3 *Connectivity constraints*

The mirror is designed with a closed backplate structure in order to strengthen its rigidity.

After the metal mirror was manufactured, it was necessary to ensure that the unmelted AlSi10Mg powders could be extracted from the interior cavities of the mirror and no powders remained in the corners of the inner cavities. The internal structure of the additively manufactured mirror is shown in Fig. 3. An airflow clearing channel is designed inside the mirror. Circular holes are cut through each pocket wall to meet the connectivity constraints. When cleaning the powders inside the mirror, the airflow can pass through a single channel, which can improve the cleaning efficiency and avoid airflow diversion. The mirror structure is unique, such that multiple inlets are used to evacuate each lattice inside the mirror to ensure the smooth discharge of the internal powder. As the size of the mirror is relatively small, no powder remains inside the mirror after an air gun performs blowing at each inlet.

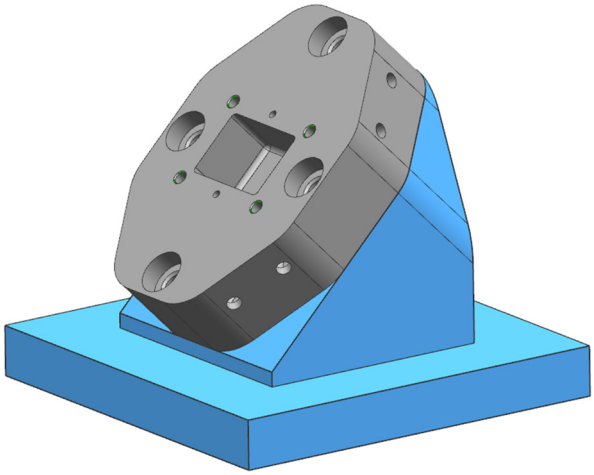

Fig. 2 Processing schematic diagram of an additively manufactured metal mirror.

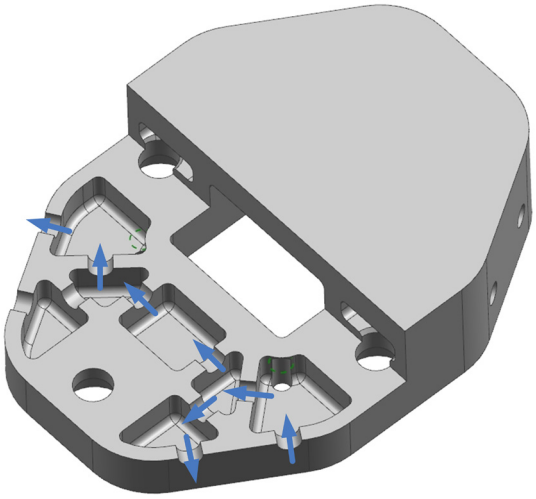

Fig. 3 Connectivity design of additively manufactured metal mirror.

2.3 *Finite Element Analysis*

The finite element analysis software was used to simulate the modal analysis and changes in the gravity-induced mirror surface for the AM mirror. The natural frequency and mode shape are important indicators to evaluate the dynamic stiffness of the structure. The natural frequency is independent of external loads. The simulation uses a restricted mode, and the restricted boundary is the actual installation position of the four-mirror screw holes on the back of the mirror. Based on the finite element analysis, the natural frequency of the mirror was determined as 4851 Hz, as shown in Fig. 4, such that the structural stiffness conforms to the requirements.

When exposed to gravity, the displacement of all nodes on the surface of the mirror was obtained via the finite element analysis. The initial coordinates and displacement of the mirror surface were fitted to obtain the deformation along the mirror surface using the MATLAB software. Figure 5 shows the surface shape analysis in the Z direction and X direction. The Zernike term 1, 2, 3 were removed (the Zernike terms 1, 2, 3 refer to piston and tip/tilt). In addition, Table 1 shows the surface accuracy of the mirror to be 0.56 nm (RMS) and 1.94 nm [peak-to-valley (PV)] in the Z direction, which conforms to the optical design requirements.

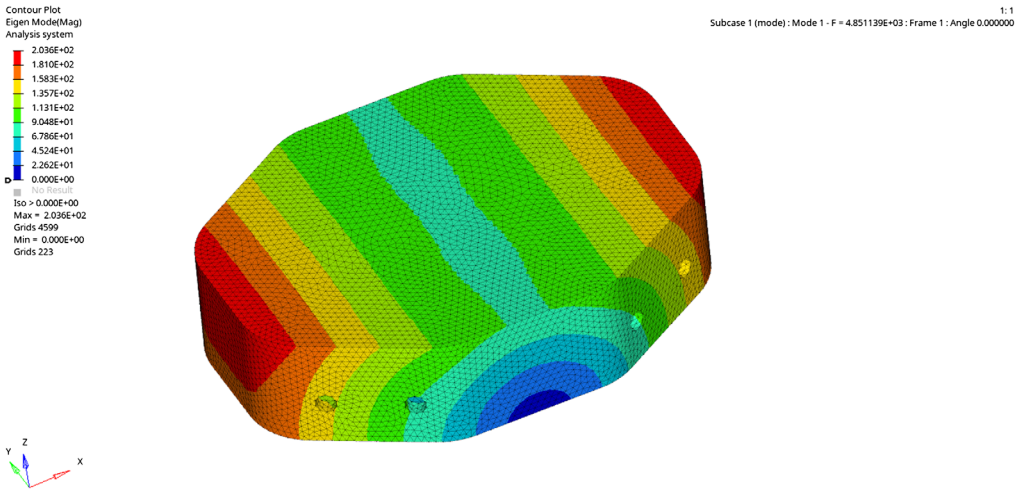

Fig. 4 Natural frequency of the mirror.

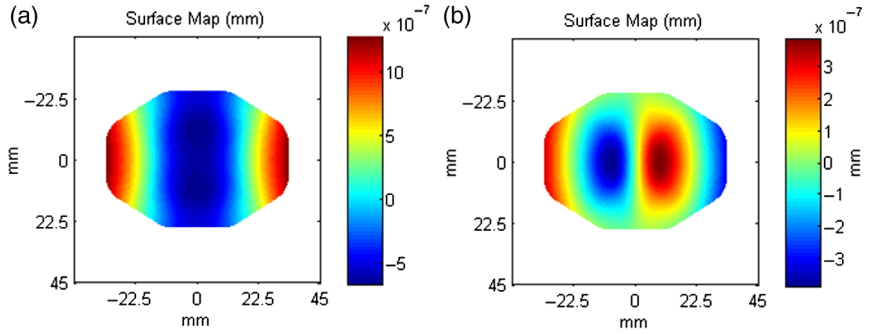

Fig. 5 Surface shape analysis in the: (a) *Z* direction and (b) *X* direction.

Table 1 Surface accuracy analysis result.

	RMS (nm)	PV (nm)
Z	0.56	1.94
X	0.17	0.77
Y	0.13	0.62

3 Fabrication of Additively Manufactured Metal Mirrors

3.1 *Additively Manufactured Metal Mirrors Process Chain*

The process chain for the manufacturing of additively manufactured metal mirrors is shown in Fig. 6. It is suitable for long wavelength applications (infrared and near-infrared).

3.2 *Additive Manufacturing Fabrication*

The material used for manufacturing the mirror was AlSi10Mg, and the material powder size was between 15 and 53 μm. The AM process parameters are given in Sec. 6. After prefabrication of the mirror base body using AM technology, the mirror was separated from the scaffolding by the wire-cutting special processing method. The deposited state of the additively fabricated mirror is shown in Fig. 7. During the SLM process, powder particles of AlSi10Mg were not completely melted, which caused the formation of void defects on the surface and inside of the mirror. The pores could be clearly seen on the surface of the mirror, which could affect the surface roughness. Therefore, densification treatment was required to eliminate macroscopic and microscopic void defects in the metal mirror, as well as to improve the densification degree of the additively fabricated mirror. After the densification treatment, the surface was processed to remove the surface pores. The weight of the additively manufactured mirror was 100 g. About 1 mm of machining was reserved on the mirror surface, back surface, and periphery of the mirror.

3.3 *Densification*

Densification is a key processing step following the AM process in the fabrication of metal mirrors. In this study, hot isostatic pressing (HIP) treatment[19] was used for densification processing and to minimize the thermal stresses of the additively fabricated mirrors. HIP technology is commonly used in the aluminum alloys and titanium alloys casting process to increase their density. It works by placing the product in a closed container, filling the container with an inert gas and then subjecting it to very high temperatures (usually close to the forging temperature of the material) and very high pressures (usually 100 to 140 MPa). The principle is that the strength of the metal material is extremely low and the plasticity is excellent at high temperature, and thus the pressure of the external gas causes the metal near the hole area to plastically deform and close the hole. Figure 8 shows an additively fabricated mirror after HIP treatment.

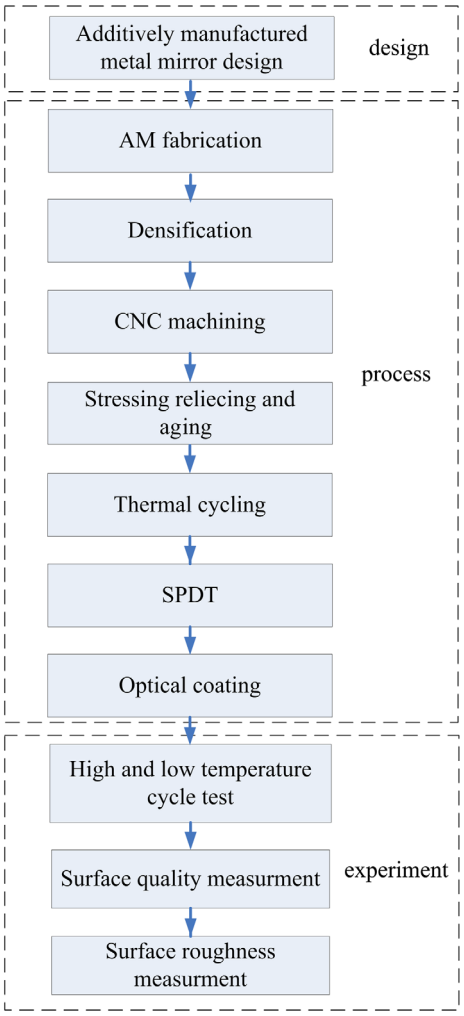

Fig. 6 Process chain for additively manufactured metal mirrors.

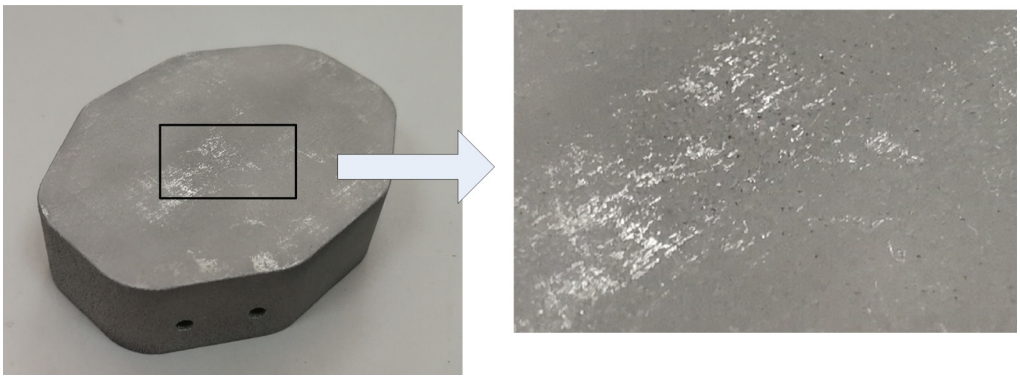

Fig. 7 Deposition state of additively fabricated mirror.

Figure 9 shows the temperature and pressure curves of the HIP treatment. Figures 9(a) and 9(b), respectively, show that its temperature range is 510 ± 25°C and its pressure range is 102 ± 2 MPa. In Fig. 9(a), the curves denoted by different colors indicate that the temperature was measured using six thermocouples. The treatment time is a minimum of 2 h. The HIP treatment requires appropriate processing parameters. Excessive processing pressure will deform the

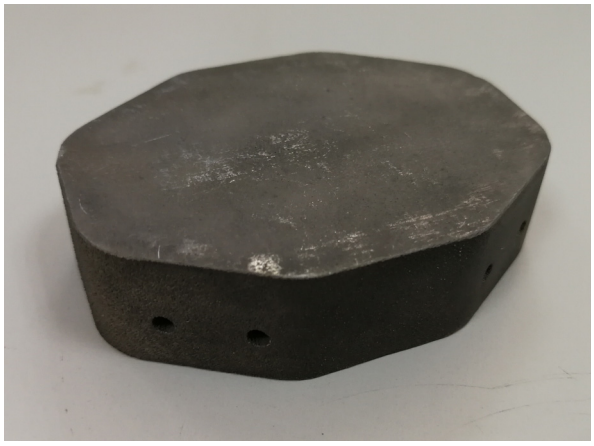

Fig. 8 Additively manufactured mirror after HIP treatment

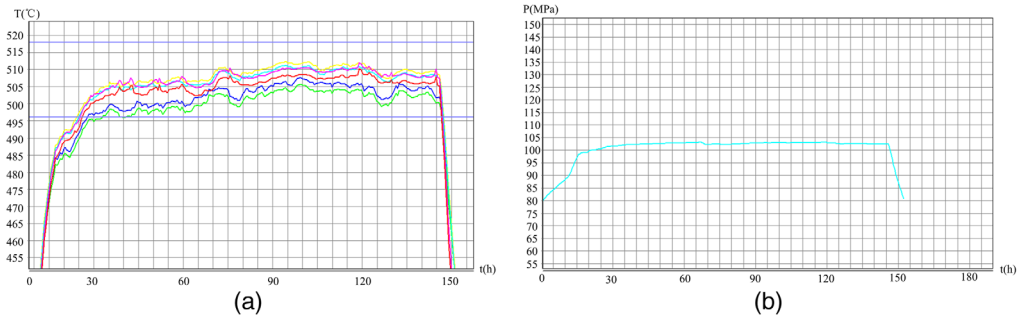

Fig. 9 Temperature and pressure curves of HIP treatment: (a) temperature curve and (b) pressure curve.

treated sample, and inadequate processing pressure will not cause densification. (see Sec. 4.4, for more detail).

3.4 *Computer Numerical Control Machining*

After the densification treatment and cleaning of the mirror, the mechanical computer numerical control (CNC) machining must be performed. All outer surfaces need to be machined.

To enable use in a harsh working environment with strong temperature changes, the stress relieving and aging methods were necessary, and they were applied during the CNC process, as described in Table 2. The quench and uphill quench steps reduce the residual stresses caused by the AM process to lower levels. The aging step is set before the semi-finishing and finishing machine processes, and it improves the strength and hardness of the mirror.

In the finishing machine step, the surface and the back of the mirror need to be milled, as shown in Fig. 10. After machining, the final weight of the AM mirror is 83 g, with a 43.7% weight reduction compared to the nonlightweight structure. This is, however, not the limit of weight reduction of this mirror.

3.5 *Thermal Cycling*

After the finishing machine step, the additively manufactured metal mirror is subjected to four sequential thermal cycle treatments to eliminate thermal stresses that may have been introduced in the semi-finishing machine and the finishing machine steps. The process is as follows: the metal mirror is placed in liquid N_2, held for 30 min, heated to 23°C, held for 30 min, heated to 160°C, held for 30 min, and cooled to 23°C. The thermal cycling temperature range is −190°C to

Table 2 Stress relieving and aging method of an additively manufactured mirror.

Steps	Stress relieving and aging method
1	Rough machine, 1 mm machining allowance
2	Solution treatment at 530 ± 5°C, hold for 2 h
3	Quench for 10 s in water at 23°C
4	Uphill quench: place in liquid N_2, hold for 30 min, then submerge in boiling water
5	Semi-finishing machine, 0.5 mm machining allowance
6	Age at 177 ± 5°C, hold for 8 h, cool with the furnace
7	Finishing machine, 0.1 mm machining allowance
8	Age at 177 ± 5°C, hold for 8 h, cool with the furnace

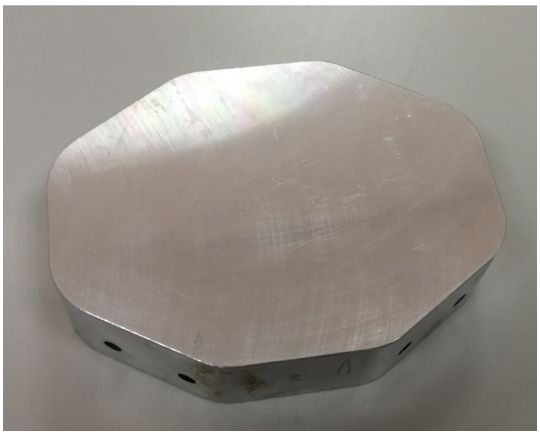

Fig. 10 Additively manufactured metal mirror after CNC machining.

$+160$°C, and the temperature changing rates do not exceed 2°C/ min. After the thermal cycle, the properties of the material become isotropic.

3.6 *Single-Point Diamond Turning Machining*

The additive manufactured mirror can be processed directly through SPDT machining. However, because of the irregular shape of the mirror, a circular transition plate was used in order to facilitate centering during the SPDT machining process. The transition plate was installed on the SPDT machining equipment by vacuum suction, and the side connected to the SPDT machining equipment had to be milled to ensure machining accuracy. The other side of the transition plate, which required SPDT machining to ensure surface flatness, was connected to the backplate of the additively manufactured mirror.

The traditional form of connection between the mirror and the transition plate is through screw fastening. Because of the unevenness between the mirror and the transition plate, the tension of the screws causes a slight deformation of the mirror. Thus, the mirror is under stress. While it can still achieve good surface quality after processing, when it is removed from the transition plate, it is released from the tension caused by the screws and returns to the free state. At this point, the surface quality of the bare mirror tends to deteriorate.

To ensure that the surface quality of the mirror remains unchanged after the removal of the transition plate, a stress-free installation form was adopted in this study. First, two cylindrical pins were used to locate the mirror on the transition plate. Then, wax was coated uniformly around the mirror, as shown in Fig. 11. Because the wax has no stress effect on the mirror during

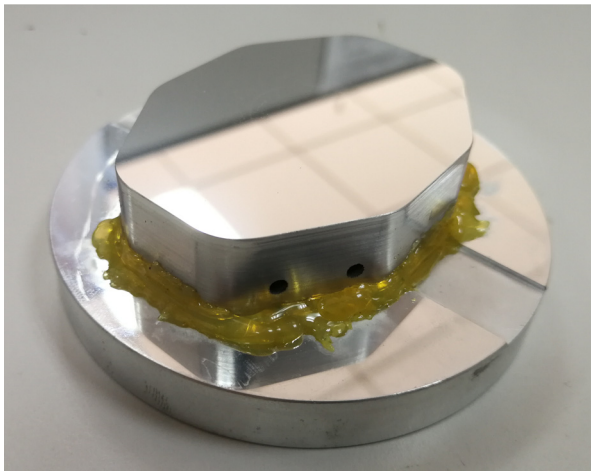

Fig. 11 Additively manufactured metal mirror after SPDT machining.

the solidification process, the mirror could be uniformly fixed on the transition plate without being affected by external force. In this manner, the surface quality of the mirror could be guaranteed when the mirror was removed from the transition plate. After SPDT machining, the transition plate was heated to 40°C to 50°C and the wax was melted. At this time, the mirror easily separated from the transition plate. A small amount of wax may remain on the side, but this residual wax can be removed with gasoline when the side of the mirror is cleaned with alcohol.

3.7 *Optical Coating*

After the SPDT step, the surface of the mirror is coated with reflective and protective layers, as seen in Fig. 12. Gold is used as the reflective coating material, and after coating, the mirror has over 95% reflectivity in the range of 3 to 5 μm. The top layer of the coating is a SiO_2 protective layer, but a film of a different material, which is suitable for harsh environments, can also be used.[20] The protective layer provides resistance to chemical corrosion and mechanical damage. The thickness of the Au coating was 220 nm, and the thickness of the protective SiO_2 layer was 170 nm. The thickness of the reflective and protective layers are typically small to ensure that, when exposed to high- and low-temperature environments, the deformation of the surface shape due to the unmatched thermal expansion coefficient is small.

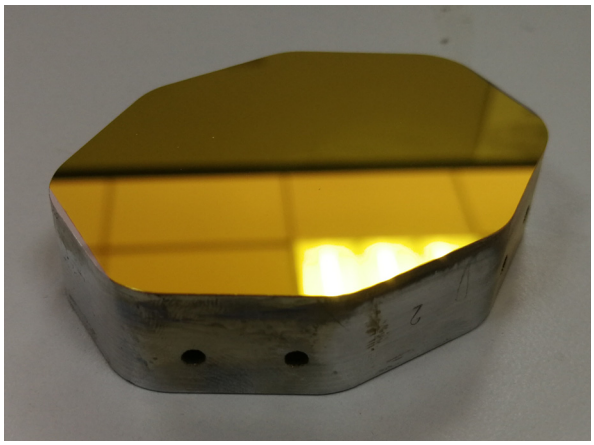

Fig. 12 Final aluminum mirror surface finish.

4 Experiment and Result Analysis

4.1 *Mirror Evaluation Method*

The mirror surface shape change is critical to the imaging quality of the optical system, making the analysis and evaluation of the surface shape change necessary. A reasonable evaluation of the surface distortion of the mirror can be performed using the PV and the RMS methods, which are the most commonly used methods. For the additively manufactured metal mirror studied in this work, the surface quality index of the bare mirror under gravity is PV $\leq \lambda/2$, RMS $\leq \lambda/10$ ($\lambda = 632.8$ nm).

The Zygo interferometer, shown in Fig. 13, was used to perform surface testing and analysis.

As shown in Fig. 14, the mirror achieved a surface quality value between 0.094 and 0.096λ (RMS), which meets the mirror surface shape requirements.

The surface accuracy of the mirror after short-term storage was verified. In a suitable storage environment, the surface accuracy of the mirror should be 0.093λ (RMS) after six months of storage, as shown in Fig. 15.

4.2 *Thermal Cycle Test*

Based on the results of the surface test, the mirror conforms to the requirements of the infrared band in a laboratory environment. To apply this additive manufactured mirror to engineering

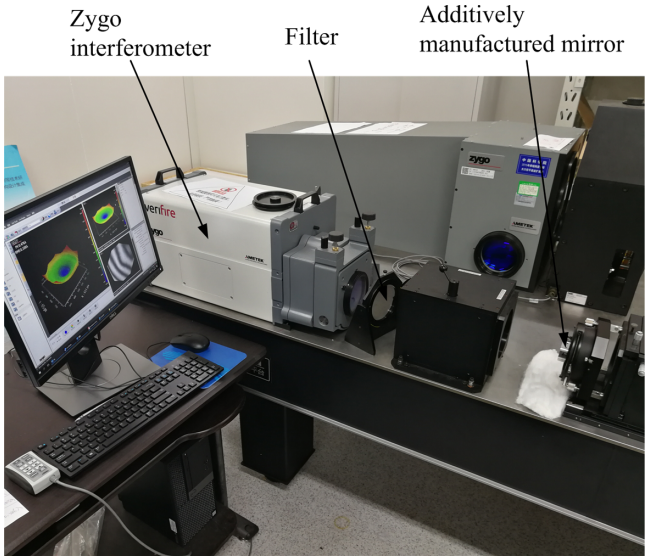

Fig. 13 Experimental equipment.

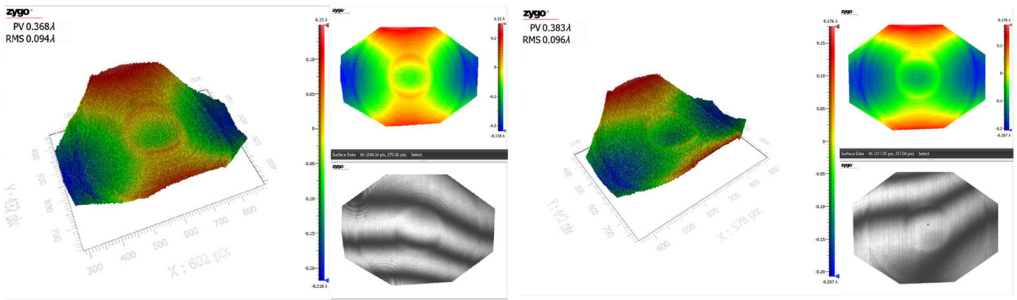

Fig. 14 Surface quality of aluminum mirror: (a) after SPDT and (b) after coating.

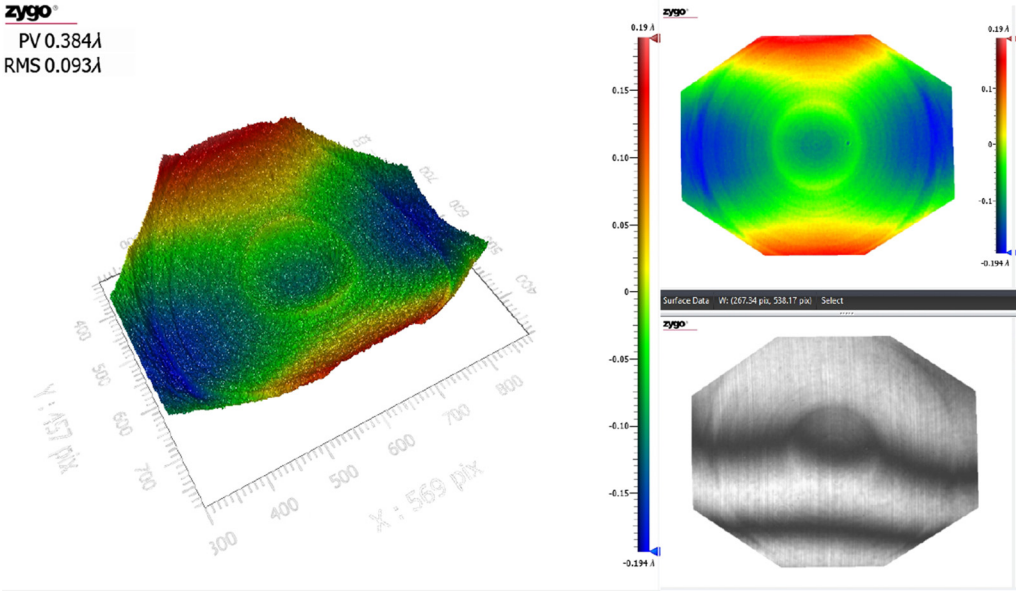

Fig. 15 Thermal cycle test conditions.

projects, especially in the aerospace field, it must be subjected to a thermal cycle test. Because of the harsh aviation working environments with their large temperature changes, the optical components in a folding optical system are required to have a wide temperature adaptation range. To evaluate the performance under different temperatures, the additively manufactured mirror was subjected to a thermal cycle test, whose conditions are shown in Fig. 16. We conducted thermal cycle tests according to industry standards, with experimental equipment capable of programming a constant temperature and humidity within a test chamber. The test consisted of cycling the mirror over the temperature range from −55°C to +70°C. The mirror is exposed to the specified operating temperature conditions and maintained at those conditions until its temperature stabilizes. The heating and cooling rates did not exceed 3°C/ min in order to prevent temperature shock. The additively manufactured metal mirror was exposed for three cycles. After the thermal cycle test, the chamber was adjusted to the standard atmospheric conditions. The optical surface quality of the metal mirror was tested before and after the thermal cycle.

The mirror surface results after the thermal cycle test are shown in Fig. 17. The surface quality of the additively manufactured mirror was PV $= 0.375\lambda$ and RMS $= 0.095\lambda$ ($\lambda = 632.8$ nm), which conforms to the basic requirements for optical mirror surface quality.

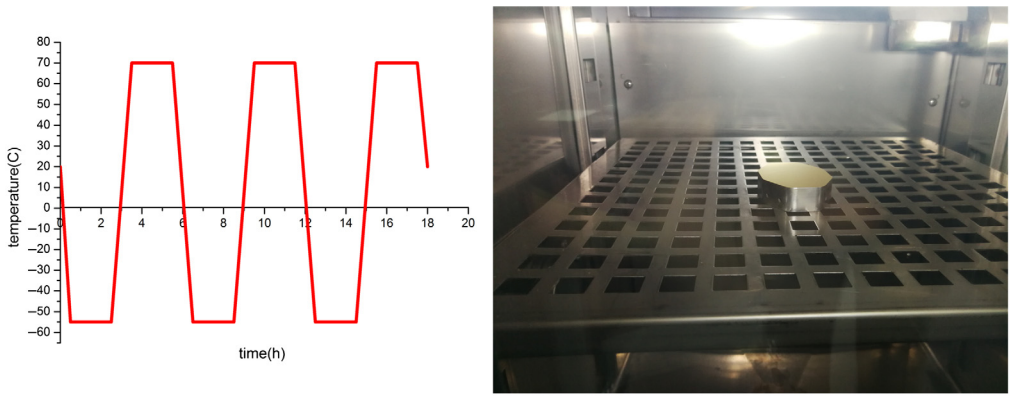

(a) (b)

Fig. 16 Thermal cycle test for the: (a) test conditions and (b) mirror in the test chamber.

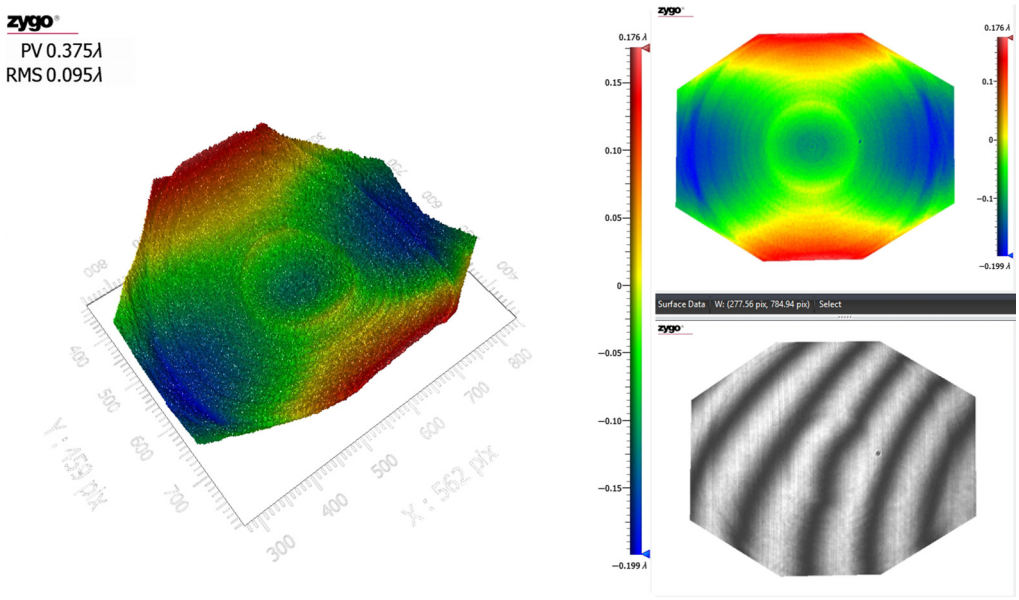

Fig. 17 Measurement value of the mirror after thermal cycling test.

The change in surface shape in high- and low-temperature environments is related to the residual stress release of the mirror. After the thermal cycle test, there was a slight change in the surface quality, which could be observed as a return to its original state. Thermal cycling tests have shown that the residual stress of the additively manufactured mirror can be released through appropriate heat treatment operations.

A summary and comparison of the measurement values of the surface quality after SPDT, coating, and the thermal cycle test are shown in the Table 3. These values demonstrate the optical stability of the additively manufactured metal mirror.

4.3 *Three-Dimensional Surface Roughness Measurement*

Surface roughness value is an important index to evaluate the surface characteristics of a mirror. The surface roughness of the mirror has a direct influence on the surface illumination. The higher the surface roughness, the greater the percentage of scattered light. In this study, the 3-D surface roughness measurement of the metal mirror was performed after the SPDT machining. The sample was tested by the white light phase-shifting interferometry method, which is a noncontact measurement method with a measurement range of 0.045 mm × 0.06 mm. Three points on the mirror surface center and edge were tested, as shown in Fig. 18. The measurement values were calculated as a mean surface roughness (Ra) of 7.244 nm for the additively manufactured metal mirror.

The total integrated scatter (TIS) theory can be used as an important parameter to evaluate the surface quality of optical components. The TIS value of the optical elements can be estimated

Table 3 Comparative summary of the surface quality at different steps.

Process step	PV	RMS	Power
After SPDT	0.368λ	0.094λ	−0.172λ
After coating	0.383λ	0.096λ	−0.062λ
After storage for 6 months	0.384λ	0.093λ	−0.022λ
After storage for 6 months and thermal cycle test	0.375λ	0.095λ	−0.014λ

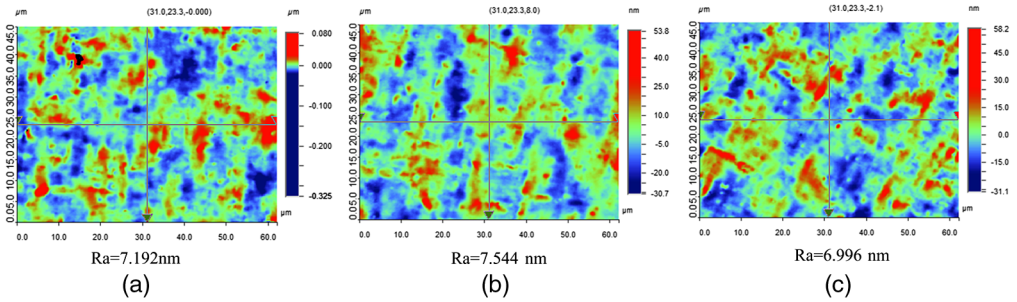

Fig. 18 Surface roughness measurements: (a) test point 1; (b) test point 2; and (c) test point 3.

using the surface roughness RMS value and can be expressed according to the TIS theory of the mirror[21] as

$$\mathrm{TIS} = 1 - \exp\left[-\left(\frac{4\pi \sin\theta\sigma}{\lambda}\right)^2\right], \tag{1}$$

where σ is the roughness (Ra) and λ is the wavelength.

When the surface roughness value (Ra) of the mirror is much smaller than the incident light wavelength and the light is incident near zero angles, the TIS can be simplified as

$$\mathrm{TIS} = \left(\frac{4\pi\sigma}{\lambda}\right)^2. \tag{2}$$

For 2500-nm (infrared band) incident light, when the surface roughness (Ra) is 7.244 nm, the TIS value is approximately 0.13%. A surface finish of this quality provides adequately low scatter. Therefore, when the transfer function meets the demand at low spatial frequencies, the additively manufactured aluminum mirrors have the potential to be applied in the infrared field, such as in wavelengths greater than 3000 nm.

4.4 *Mirror Microstructure*

4.4.1 *Scanning electron microscopy test*

To deduce whether the densification treatment of the additively manufactured metal mirrors is effective, the AlSi10Mg specimens were processed for microstructure tests. The AlSi10Mg specimens in the deposited and HIP states were milled and polished. The surface was then etched using a Keller reagent (2.5 mL HNO_3, 1.5 mL HCl, 1 mL HF, and 100 mL H_2O) for 30 s. The surface topography of the specimens was obtained using scanning electron microscopy (SEM) equipment. The SEM results are shown in Fig. 19. In Fig. 19(a), the AlSi10Mg deposited state specimen was magnified 3300 times, and it can be clearly seen that the specimen has a void that is approximately 20 μm × 5 μm in size. Unmelted AlSi10Mg powder particles could be seen on the left of the specimen. Figure 19(b) shows the AlSi10Mg specimen that underwent HIP treatment. No apparent voids can be observed in the field of view, and the structures can be seen to be more compact in the HIP state. Comparing the two SEM results, the HIP densification process is very effective for the densification of additively manufactured aluminum mirrors.

4.4.2 *Micro-focus computer tomography test*

To more clearly demonstrate the increase in the density of AM by HIP, computer tomographic (CT) scans were used to test the porosity before and after the HIP. The test equipment is diondo-d2 high-resolution all-round microfocus CT detection system. Figure 20 shows the pore distribution inside the sample before and after the HIP treatment. The dimensions of the two prototypes are approximately equal. It can be clearly seen that the porosity inside the sample

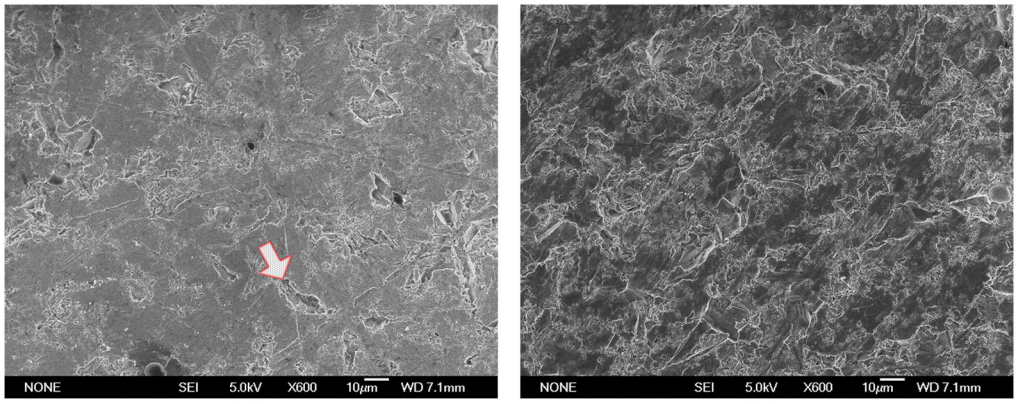

(a) (b)

Fig. 19 Microstructure of AlSi10Mg specimens: (a) deposited state and (b) HIP state.

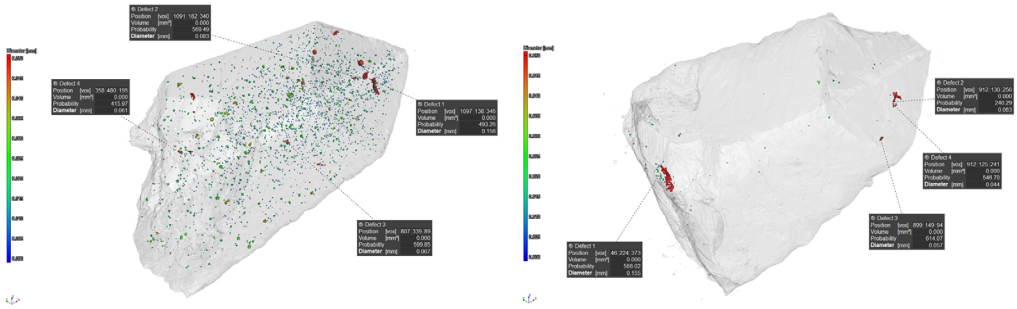

(a) (b)

Fig. 20 CT test results of AlSi10Mg specimens: (a) deposited state and (b) HIP state.

was reduced after the HIP treatment. After statistical calculation, the porosity before HIP was 0.092% and the porosity after HIP was 0.005%.

5 Conclusions

In this study, an aluminum mirror design and fabrication method based on AM technology, which can relatively quickly and easily prepare metal mirrors, is proposed based on the volume and weight requirements of the optical folding system used in modern aviation. An aluminum mirror design method based on AM technology process was introduced, and an additively manufactured metal mirror process chain was studied. The experimental results show that the surface shape deviation was 0.384λ (PV) and 0.093λ (RMS) ($\lambda = 632.8$ nm) for a bare metal mirror. The surface roughness (Ra) of the mirror is better than 8 nm. After the thermal cycle test, the surface quality did not change significantly, thus meeting the basic requirements of aviation environment adaptability. The research presented in this paper provides a reference for a metal mirror with good aviation environment adaptability for applications in the infrared band.

6 Appendix A: Machine Parameters

Machine model: EOS M280
Powder: AlSi10Mg
Laser: Yb-fiber
Laser power: 400 W
Laser fiber diameter: 100 to 500 μm

Laser wavelength:1060 to 1110 nm
Scanning speed: 980 mm/s
Scan spacing: 0.11 mm
Controlled atmosphere: argon
Stops during build: none

Acknowledgments

The authors are thankful for the support from the Key Laboratory of Airborne Optical Imaging and Measurement, Changchun Institute of Optics, Fine Mechanics and Physics, Chinese Academy of Sciences. The authors declare no conflicts of interests. This research was funded by the National Key Research and Development Program of China (No. 2017YFC0822403).

References

1. S. H. Philip, "Development of lightweight mirror technology for the next generation space telescope," *Proc. SPIE* **4451**, 1–4 (2001).
2. M. Y. Chen et al., "Replication of lightweight mirrors," *Proc. SPIE* **7425**, 74250S (2009).
3. L. E. Matson and M. Y. Chen, "Enabling materials and processes for large aerospace mirrors," *Proc. SPIE* **7018**, 70180L (2008).
4. K. S. Woodard et al., "Cost-effective lightweight mirrors for aerospace and defense," *Proc. SPIE* **9451**, 94511W (2015).
5. S. Risse et al., "Novel TMA telescope based on ultra precise metal mirrors," *Proc. SPIE* **7010**, 701016 (2008).
6. J. Zhang et al., "A review of selective laser melting of aluminum alloys: processing, microstructure, property and developing trends," *J. Mater. Sci. Technol.* **35**(2), 270–284 (2019).
7. E. Brandl et al., "Additive manufactured AlSi10Mg samples using selective laser melting (SLM): microstructure, high cycle fatigue, and fracture behavior," *Mater. Des.* **34**, 159–169 (2011).
8. H. Herzog et al., "Optical fabrication of lightweighted 3D printed mirrors," *Proc. SPIE* **9573**, 957308 (2016).
9. R. Ter Horst et al., "Directly polished lightweight aluminum mirror," *Proc. SPIE* **7018**, 701808 (2008).
10. C. Atkins et al., "Topological design of lightweight additively manufactured mirrors for space," *Proc. SPIE* **10706**, 107060I (2018).
11. M. Sweeney et al., "Application and testing of additive manufacturing for mirrors and precision structures," *Proc. SPIE* **9574**, 957406 (2015).
12. S. Scheiding et al., "Method for manufacturing a mirror comprising at least one cavity and optical mirror," WO, EP2739998 (2014).
13. J. Casstevens, "Additive manufactured very light weight diamond turned aspheric mirror," NASA SBIR/STTR Technologies (2017).
14. K. S. Woodard and B. H. Myrick, "Progress on high-performance rapid prototype aluminum mirrors," *Proc. SPIE* **10181**, 101810T (2017).
15. K. S. Woodard et al., "Optimum selection of high performance mirror substrates for diamond finishing," *Proc. SPIE* **9822**, 98220C (2016).
16. N. Heidler et al., "Additive manufacturing of metal mirrors for TMA telescope," *Proc. SPIE* **10692**, 106920C (2018).
17. M. Leary et al., "Optimal topology for additive manufacture: a method for enabling additive manufacture of support-free optimal structures," *Mater. Des.* **63**(6), 678–690 (2014).
18. E. Hilpert et al., "Design, additive manufacturing, processing, and characterization of metal mirror made of aluminum silicon alloy for space applications," *Opt. Eng.* **58**(9), 092613 (2019).
19. M. N. Gussev et al., "Influence of hot isostatic pressing on the performance of aluminum alloy fabricated by ultrasonic additive manufacturing," *Scr. Mater.* **145**, 33–36 (2018).

20. C. Hu et al., "New design for highly durable infrared-reflective coatings," *Light: Sci. Appl.* **7**(4), 17175 (2017).
21. E. Friedman and J. L. Miller, *Photonice Rules of Thumb*, McGraw-Hill, New York (2003).

Songnian Tan is an assistant professor in Key Laboratory of Airborne Optical Imaging and Measurement, Chinese Academy of Sciences. He received his BS and MS degrees from Harbin Institute of Technology in 2012 and 2014. His current research interests include photovoltaic platform and metal mirror manufacturing.

Yalin Ding received a bachelor's degree from Jilin University of Technology in 1987 and a master's degree from Northeastern University in 1994. He is mainly engaged in the research of the optical-mechanical structure technology of aerial remote sensing instruments and the stable imaging technology under dynamic conditions of aircraft. He has authored and coauthored over 100 journal and conference articles.

Yongsen Xu graduated with a PhD degree in optical engineering from Changchun Institute of Optics, Fine Mechanics and Physics, Chinese Academy of Sciences, in 2009. He is a research scientist in the Key Laboratory of Airborne Optical Imaging and Measurement, Chinese Academy of Sciences. His current work topic is related to aerial imaging and measurement research.

Lei Shi graduated with a PhD in mechanical engineering from Jilin University in 2009. He is a research scientist in the Key Laboratory of Airborne Optical Imaging and Measurement, Chinese Academy of Sciences. His current work topic is related to aerial imaging and measurement research.